

POYNTING JETS FROM ACCRETION DISKS: MAGNETOHYDRODYNAMIC SIMULATIONS

G. V. USTYUGOVA,¹ R. V. E. LOVELACE,^{2,3} M. M. ROMANOVA,^{2,3} H. LI,² AND S. A. COLGATE²

Received 2000 April 11; accepted 2000 July 31; published 2000 September 6

ABSTRACT

The powerful narrow jets observed to emanate from many compact accreting objects may arise from the twisting of a magnetic field threading a differentially rotating accretion disk that acts to extract magnetically the angular momentum and energy from the disk. Two main regimes have been discussed, *hydromagnetic outflows*, which have a significant mass flux and which have the energy and angular momentum carried by both the matter and the electromagnetic field, and *Poynting outflows*, in which the mass flux is negligible and the energy and angular momentum are carried predominantly by the electromagnetic field. Recent simulation studies have focused almost exclusively on hydromagnetic outflows. Here we consider a Keplerian disk initially threaded by a dipole-like poloidal magnetic field. We present the first MHD simulation results establishing that a quasi-stationary collimated Poynting jet arises from the inner part of the disk while a steady uncollimated hydromagnetic outflow arises in the outer part of the disk.

Subject headings: accretion, accretion disks — black hole physics — magnetic fields — MHD — plasmas

1. INTRODUCTION

Powerful, highly collimated, oppositely directed jets are observed in active galaxies and quasars (see, e.g., Bridle & Eilek 1984), and in old compact stars in binaries (Mirabel & Rodríguez 1994; Eikenberry et al. 1998). Furthermore, emission-line jets are seen in young stellar objects (Mundt 1985; Bührke, Mundt, & Ray 1988). Different ideas and models have been put forward to explain astrophysical jets (see reviews by Begelman, Blandford, & Rees 1984; Bisnovatyi-Kogan 1993, and Lovelace, Ustyugova, & Koldoba 1999).

An ordered magnetic field is widely thought to have an essential role in jet formation from a rotating accretion disk. Two main regimes have been considered in theoretical models, the *hydromagnetic regime*, in which the energy and angular momentum are carried by both the electromagnetic field and the kinetic flux of matter, and the *Poynting regime*, in which the energy and angular momentum outflows from the disk are carried predominantly by the electromagnetic field. The hydromagnetic outflows arise when the inclination of an ordered magnetic field away from the z -axis θ at the disk surface is larger than $\sim 30^\circ$; under this condition, the centrifugal force along a field line extending out of a Keplerian disk can be of the order of the gravitational force that results in the easy outflow of matter from the disk surface (Blandford & Payne 1982). On the other hand, when $\theta < 30^\circ$, matter outflow from the disk may be strongly suppressed by the vertical gravitational force, and a Poynting jet can occur (Lovelace 1976; Blandford 1976). The jets from young stellar objects have large mass outflow rates that may be understood in terms of hydromagnetic outflows (Pudritz & Norman 1986; Königl & Ruden 1993). On the other hand, extragalactic jets and the jets from microquasars can be interpreted in terms of Poynting jets (Blandford 1993; Romanova & Lovelace 1997; Lovelace et al. 1999).

Recent progress in understanding the origin of *hydromagnetic* jets has come from MHD simulations of outflows from disks (Bell 1994; Ustyugova et al. 1995, 1999; Koldoba et al.

1995; Romanova et al. 1997, 1998; Meier et al. 1997; Ouyed & Pudritz 1997; Krasnopolsky, Li, & Blandford 1999; Koide et al. 2000). Stationary Poynting flux-dominated outflows were found by Romanova et al. (1998) in a study of the opening of magnetic loops threading a Keplerian disk. Theoretical studies have developed detailed models for Poynting jets from accretion disks (Lovelace, Wang, & Sulkanen 1987; Colgate & Li 2000; Lynden-Bell 1996; Romanova & Lovelace 1997; Levinson 1998; H. Li, R. V. E. Lovelace, J. M. Finn, & S. A. Colgate 2000, in preparation).

The goal of this Letter is to investigate the Poynting jets numerically. We envision that the inner part of the disk is threaded by a magnetic field loop configuration that extends into a high-temperature disk corona. The differential rotation of the loop footpoints on the disk causes the loop to expand and open, thus creating a new field structure (Newman, Newman, & Lovelace 1992) and Poynting outflows (Romanova et al. 1998). The timescale for opening of the loop is of the order of the disk rotation period, which is much shorter than both the accretion timescale and the timescale for radial slippage of field lines in the disk (Lovelace, Newman, & Romanova 1997). Compared with Romanova et al. (1998), we consider a dipole-like magnetic field threading the disk and a *much larger* computational region that allows us to study the outflow collimation. We find that a quasi-stationary collimated Poynting jet arises from the inner part of the disk *and* that a steady uncollimated hydromagnetic outflow arises from the outer disk. In § 2 we describe the simulations, in § 3 the results, and in § 4 we discuss the results.

2. MHD SIMULATIONS

We solve the full system of MHD equations for axisymmetric, nonrelativistic, ideal magnetohydrodynamic flows, including all three components of the flow velocity \mathbf{v} and magnetic field \mathbf{B} and the gravitational acceleration of the central object (see, e.g., Ustyugova et al. 1999). The plasma equation of state is $p = \text{const } \rho^\gamma$ with $\gamma = 5/3$. The disk is treated as a boundary condition, as first proposed by Ustyugova et al. (1995).

The magnetic field is $\mathbf{B} = B_p + B_\phi \hat{\phi}$, with $B_p = B_r \hat{r} + B_z \hat{z}$ in cylindrical coordinates. Because $\nabla \cdot \mathbf{B} = 0$, $\mathbf{B} = \nabla \times \mathbf{A}$, where \mathbf{A} is the vector potential. Consequently, $B_r = -(1/r) \times$

¹ Keldysh Institute of Applied Mathematics, Russian Academy of Sciences, Miusskaya Square 4, Moscow, 125047, Russia.

² Theoretical Astrophysics, T-6, MS B288, Los Alamos National Laboratory, Los Alamos, NM 87545.

³ Department of Astronomy, Cornell University, 512 Space Sciences Building, Ithaca, NY 14853-6801; rv11@cornell.edu.

$\partial\Psi/\partial z$, and $B_z = (1/r)\partial\Psi/\partial r$, where $\Psi(r, z) \equiv rA_\phi(r, z)$. The $\Psi(r, z) = \text{const}$ lines label the poloidal field lines; i.e., $(\mathbf{B} \cdot \nabla)\Psi = (\mathbf{B}_p \cdot \nabla)\Psi = 0$. The magnetic flux through a horizontal circular disk of radius r is $2\pi\Psi(r, z)$.

The initial magnetic field threading the disk and extending into the disk's corona is assumed to have a dipole-like form, as shown in the bottom left-hand panel of Figure 1. Such a field can arise from a disk dynamo that is driven by star-disk collisions, as discussed by V. Pariev, J. M. Finn, & S. A. Colgate (2000, in preparation), or it can arise from an interstellar magnetic field that is advected inward by the accretion flow. On the surface of the disk, we take $\Psi(r, z = 0) = (3/2)^{3/2} \times (r/r_0)^2 \Psi_{\text{max}} f(r) [\frac{1}{2} + (r/r_0)^2]^{-3/2}$, where r_0 is the radius of the O -point of the initial magnetic field where the flux function has its maximum value Ψ_{max} . The function $f(r) = 1 - (r - r_0)^2 / (R_{\text{max}} - r_0)^2$ is introduced so that the flux coming out of the disk for $0 \leq r \leq r_0$ goes back into the disk for $r_0 \leq r \leq R_{\text{max}}$; i.e., $\Psi(R_{\text{max}}, 0) = \Psi(0, 0) = 0$. The magnetic field at the center of the disk is $B_z(0, 0) = 6\sqrt{3}\Psi_{\text{max}}/r_0^2$. The initial $\Psi(r, z > 0)$ is calculated by solving $\Delta^* \Psi = 0$ [with $\Delta^* \equiv \partial^2/\partial r^2 - (1/r)\partial/\partial r + \partial^2/\partial z^2$] by successive over-relaxation, with boundary conditions $\Psi(r, 0)$ as given and $\Psi(R_{\text{max}}, z) = \Psi(r, Z_{\text{max}}) = \Psi(0, z) = 0$.

We measure distances in units of the O -point radius r_0 , Ψ in units of its value at $(r_0, 0)$, i.e., Ψ_{max} , and the magnetic field strength in units of Ψ_{max}/r_0^2 . The computational region, $r = 0$ to R_{max} , $z = 0$ to Z_{max} , is taken to have $R_{\text{max}} = Z_{\text{max}} \approx 10r_0$. We use a 100×100 inhomogeneous grid with Δr_j and Δz_k growing with the distances of r and z geometrically as $\Delta r_j = \Delta r_1 q^j$ and $\Delta z_k = \Delta z_1 q^k$, with $q = 1.03$ and $\Delta r_1 = \Delta z_1 = 0.05r_0$.

Initially, the corona of the disk is in isothermal equilibrium without rotation. At $t = 0$, the disk starts to rotate with a Keplerian velocity $v_\phi(r, 0) = r\Omega_K$, where $\Omega_K = (GM)^{1/2}/(r^2 + r_i^2)^{3/4}$, where the smoothing length $r_i = 0.2r_0$ is interpreted as the inner radius of the disk. The smoothed gravitational potential is $-GM/(r_i^2 + r^2)^{1/2}$.

On the disk surface, we adopt a modification of the boundary conditions of Ustyugova et al. (1999). Two of the boundary conditions are the result of the tangential electric field (\mathbf{E}'), in the frame rotating with the disk (at the Keplerian velocity) equaling zero; B_z at the disk surface is time-independent, whereas B_r and B_ϕ at the surface vary with time.⁴ At the disk surface, these two conditions give $v_r = \kappa B_r$ and $v_\phi = r\Omega_K + \kappa B_\phi$, where $\kappa = v_z/B_z$. Two further boundary conditions fix the entropy of the plasma coming out of the disk to be $s_d(r)$ and the density of the outflowing plasma to be $\rho_d(r)$. If v_z at the disk surface, calculated by solving the MHD equations in the computational region, increases to the point where it is larger than the slow magnetosonic speed in the z -direction at the disk's surface c_{smz} , then we clamp it to be equal to c_{smz} . This condition represents a limit on the mass efflux ρv_z from the disk. For a sub-slow magnetosonic outflow from the disk ($v_z < c_{\text{smz}}$), we have four boundary conditions, whereas when $v_z = c_{\text{smz}}$, we have five boundary conditions.

On the outer boundaries, we take the “free” boundary conditions $\partial F_j/\partial n = 0$ on all scalar variables, *except* for the toroidal magnetic field. For this field component, we take

⁴ The statement in the first paragraph of § 3.3 of Romanova et al. (1998) that the poloidal components of the magnetic field at the disk surface (B_r, B_z) are fixed is a misstatement. The correct statement is that the B_z component at the disk surface is fixed, while the B_r and B_ϕ components are allowed to change.

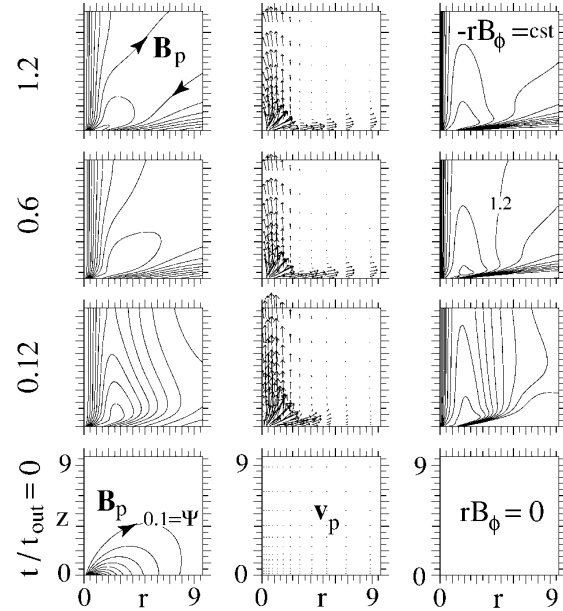


FIG. 1.—Time evolution of dipole-like field threading the disk from the initial configuration $t = 0$ (bottom panels) to the final quasi-stationary state $t = 1.2t_{\text{out}}$, where t_{out} is the rotation period of the disk at the outer radius R_{max} of the simulation region. The left-hand panels show the poloidal field lines that are the same as $\Psi(r, z) = \text{const}$ lines; Ψ is normalized by Ψ_{max} , and the spacing between the lines is 0.1. The middle panels show the poloidal velocity vectors \mathbf{v}_p . The right-hand panels show the constant lines of $-rB_\phi(r, z) > 0$ in units of Ψ_{max}/r_0 , and the spacing between the lines is 0.1.

$[\mathbf{B}_p \cdot \nabla(rB_\phi)] = 0$ on the outer boundaries, which was shown by Ustyugova et al. (1999) to avoid artificial collimation that can come from using the “free” boundary condition on rB_ϕ . These conditions allow the matter and the Poynting flux to flow out freely through these boundaries.

3. RESULTS

For the case we discuss in detail, the strength of the poloidal magnetic field at the inner radius of the disk corresponds to $(v_{\text{Ap}}/v_K)_i = 16.5$ and $(c_s/v_K)_i = 1$, where $v_{\text{Ap}} \equiv |\mathbf{B}_p|/(4\pi\rho)^{1/2}$. The subscript i indicates the evaluation at the inner radius of the disk $r = r_i$ on the disk surface, where $r_i = 6GM/c^2 \approx 8.9 \times 10^{13}$ cm ($M/10^8 M_\odot$) (for a Schwarzschild black hole). In the midplane of the disk, $(v_{\text{Ap}}/v_K)_{z=0}$ is less than or much less than unity. Different radial profiles of c_s on the disk surface have been used with similar results, including $c_s/v_K = \text{const}$ and $c_s = \text{const}$; the density profiles on the disk surface have been obtained as in Ustyugova et al. (1999). At r_i , $v_{\text{Ki}} \approx 0.73 \times 10^{10}$ cm s⁻¹, and the disk rotation period at r_i is $t_i \equiv 2\pi r_i/v_{\text{Ki}} \approx 0.89$ days ($M/10^8 M_\odot$). The period of rotation of the disk at the outer radius of the simulation region t_{out} is a factor $(R_{\text{max}}/r_i)^{3/2}/2^{3/4} \sim 200$ longer than t_i for $r_i = 0.2r_0$ and $R_{\text{max}} \approx 10r_0$.

Figure 1 shows the temporal evolution—from the bottom to the top—of the initial dipole-like field. The differential rotation of the disk acts to twist the magnetic field, and this “pumps” the toroidal magnetic flux and energy into the disk corona, and the field loops “inflate.” This behavior of the magnetic field loops on the surface of the Sun, which is the result of footpoint twisting, is well known from the works of Aly (1984) and

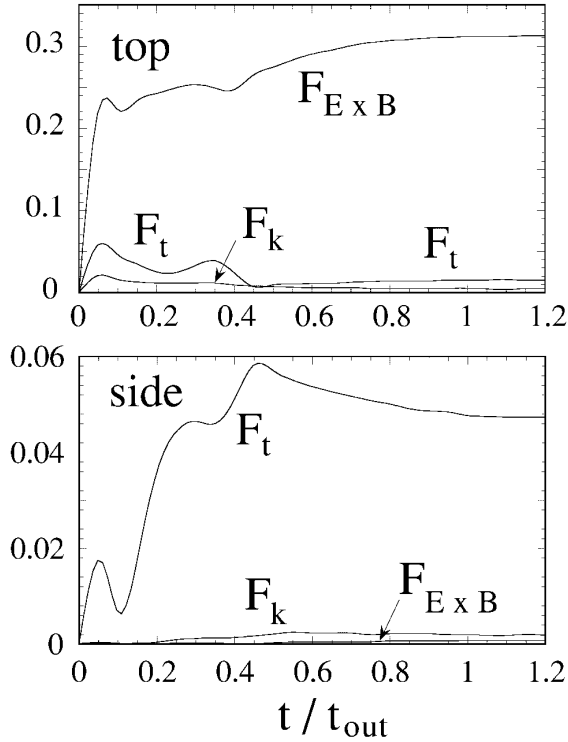


FIG. 2.—Energy fluxes—Poynting $F_{E \times B}$, thermal F_t , and kinetic F_k —through the top boundary $z = Z_{\max}$ (top) and through the side boundary $r = R_{\max}$ (bottom) as a function of time measured in units of the rotation period of the disk t_{out} at the outer radius of the simulation region R_{\max} . The scales for the two panels are the same but arbitrary. The top panel describes the Poynting jet that, for long times, has an electromagnetic energy flux $c \int d^2r (\mathbf{E} \times \mathbf{B})_z / 4\pi$ that is ≈ 16.5 times that carried by the matter. In this ideal MHD flow, $\mathbf{E} + \mathbf{v} \times \mathbf{B}/c = 0$. The ratio of the total power flow in the Poynting jet to that in the hydromagnetic outflow is ≈ 6.5 . The ratio of the mass flux out the side boundary to that out the top is ≈ 13 .

Sturrock (1991) on force-free magnetic fields. A plot of the forces along a field line that originates in the inner part of the disk and goes into the Poynting jet shows that the pressure force is dominant for distances $\lesssim r_0$ from the disk, while at larger distances, the magnetic force is dominant.

For long times $t \gtrsim t_{\text{out}}$, the corona evolves into a quasi-stationary configuration consisting of (1) an axial-collimated Poynting jet, with a steady outflow of energy and of toroidal flux originating from the disk field lines within the O -point, and (2) a steady fan-shaped, matter-dominated outflow originating from the disk field lines outside the O -point. At the outer boundaries, the flow velocities are larger than the escape speed; the flow velocity of the Poynting jet is less than the Alfvén speed, while that of the hydromagnetic outflow is greater than the Alfvén speed. We have verified that the flow and field configurations found here are independent of the location of the outer boundaries by calculations with larger (R_{\max}, Z_{\max}) . Figure 2 shows the different contributions to the energy fluxes through the top and side boundaries.

The Poynting jet carries a net axial current [negative for $B_z(r < r_0, 0) > 0$]. This current flows into the disk, radially outward within the disk, outward in the hydromagnetic outflow, and forms a closed path at a large distance from the disk. Figure 3 shows the radial profiles of B_z , B_ϕ , and $rB_\phi = (2/c)I_z(r)$ across

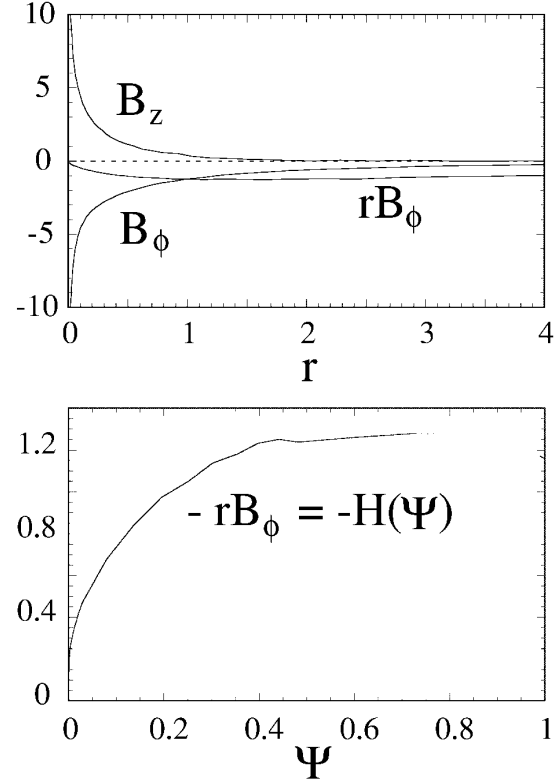


FIG. 3.—Top: Radial profiles of the field components of the Poynting jet at $z = Z_{\max}/2$ and $t/t_{\text{out}} = 1.2$. (The plot has been stopped at $r = 4$ so as to make the field profiles within the jet visible. For $r > 4$, $rB_\phi = \text{const}$ and $B_z = 0$.) Bottom: Numerically derived dependence of rB_ϕ on Ψ , with Ψ in units of Ψ_{\max} , r in units of r_0 , the O -point radius, and B in units of Ψ_{\max}/r_0^2 . The azimuthal angle of a field line ϕ for $r \lesssim r_0$ is given by $d\phi/dz \approx -\text{const}/r(\Psi)$ in that $B_z \sim -B_\phi \propto r^{-2.5}$ and $\Psi \propto r^{3.4}$. To a good approximation, the Poynting jet for $z \geq 0$ is force-free with $\mathbf{J} \times \mathbf{B} = 0$ (Gold & Hoyle 1960) so that the flux function Ψ obeys the Grad-Shafranov equation $\Delta^* \Psi = -H(dH/d\Psi)$, where $H(\Psi) = rB_\phi(r, z)$ (H. Li, R. V. E. Lovelace, J. M. Finn, & S. A. Colgate 2000, in preparation).

the jet in the quasi-stationary state, where $I_z(r)$ is the axial current within the radius r . The B_z component acts to expand the jet radially, while B_ϕ acts to confine it. The radial-force balance across the jet $\partial(B_z^2)/\partial r + (1/r^2)\partial(r^2 B_\phi^2)/\partial r = 0$ is accurately satisfied by these field profiles. The increase of B_ϕ and B_z with decreasing r reflects the increase of the twist of the field lines around the z -axis, and this results from the increase of $\Omega_K(r)$. The angle between the poloidal field and the z -axis θ is less than 30° over most of the inner disk ($r < r_0$) surface. At the same time, the toroidal field of the jet acts to anticollimate or “squash” the outflow from the outer disk ($r > r_0$) onto the disk surface, and $\theta > 60^\circ$ over most of this range of r .

Quasi-stationary Poynting jets from the two sides of the disk within r_0 give an energy outflow per unit radius of the disk $d\dot{E}_B/dr = rv_K(-B_\phi B_z)_h$, where the subscript h indicates the evaluation at the top surface of the disk. This outflow is $\sim r_0 d\dot{E}_B/dr \sim v_K(r_0)(\Psi_{\max}/r_0)^2 \sim 10^{45}$ (ergs s^{-1}) $r_{015}^{3/2} (M_8)^{1/2} \times [B_z(0)/6 \text{ kG}]^2$, where r_{015} is in units of 10^{15} cm and M_8 is in units of $10^8 M_\odot$. This formula agrees approximately with the values derived from the simulations. The jets also give an outflow of angular momentum from the disk that causes disk accretion (without viscosity) at the rate of $\dot{M}_B(r) \equiv -2\pi\Sigma v_r =$

$-2(r^2/v_k)(B_\phi B_z)_h \sim 2\Psi_{\max}^2/[r_0^2 v_k(r_0)]$, where Σ is the disk's surface mass density (Lovelace et al. 1997). The Poynting jet has a net axial momentum flux of $\dot{P}_z = \frac{1}{4} \int r dr (B_\phi^2 - B_z^2) \sim 0.5(\Psi_{\max}/r_0)^2$, which acts to drive the jet outward through an external medium. Furthermore, the Poynting jet generates toroidal magnetic flux at the rate $\dot{\Phi}_z \sim -12[v_k(r_0)/r_0]\Psi_{\max}$ (H. Li, R. V. E. Lovelace, J. M. Finn, & S. A. Colgate 2000, in preparation).

4. DISCUSSION

The Poynting jet is quasi-stationary and approximately force-free so that particles are not directly accelerated in its \mathbf{E} - and \mathbf{B} -fields. In a more complete picture, the jet is time-dependent: it has a "front" consisting of internal and external shocks where it pushes through the interstellar medium or pushes into the magnetic field remaining from a prior jet outburst (Romanova & Lovelace 1997; Levinson 1998). Front propagation through a homogeneous external medium is naturally focused toward the axis because of the falloff of the jet's magnetic pressure with radius (which is due to the falloff of the poloidal and toroidal magnetic fields with r). Particle acceleration in the shocks or in field reconnection events at a propagating front makes the jet visible and may explain the outbursts of blazars (Romanova & Lovelace 1997; Levinson 1998; Romanova 1999).

Furthermore, for long timescales, the Poynting jet is time-

dependent because of the angular momentum it extracts from the inner disk ($r < r_0$). This loss of angular momentum leads to a "global magnetic instability" and the collapse of the inner disk (Lovelace et al. 1997). An approximate model of this collapse can be made if the inner disk mass M_d is concentrated near the O -point radius $r_0(t)$, if the field-line slippage through the disk is negligible (Lovelace et al. 1997), $\Psi_{\max} = \text{const}$, and if $(-rB_\phi)_{\max} \sim \Psi_{\max}/r_0(t)$ (as found here). Then $M_d dr_0/dt = -2\Psi_{\max}^2(GMr_0)^{-1/2}$. If t_i denotes the time at which $r_0(t_i) = r_i$ (the inner radius of the disk), then $r_0(t) = r_i[1 - (t - t_i)/t_{\text{coll}}]^{2/3}$ for $t \leq t_i$, where $t_{\text{coll}} = (GM)^{1/2} M_d r_i^{3/2} / (3\Psi_{\max}^2)$ is the timescale for the collapse of the inner disk. [Note that the timescale for r_0 to decrease by a factor of 2 is $\sim t_i(r_0/r_i)^{3/2} \gg t_i$ for $r_0 \gg r_i$.] The power output to the Poynting jets is $\dot{E}(t) = (2/3)(\Delta E_{\text{tot}}/t_{\text{coll}})[1 - (t - t_i)/t_{\text{coll}}]^{-5/3}$, where $\Delta E_{\text{tot}} = GMM_d/2r_i$ is the total energy of the outburst. Roughly, $t_{\text{coll}} \sim 2 \text{ days } M_8^2 (M_d/M_\odot) (6 \times 10^{32} \text{ G cm}^2/\Psi_{\max}^2)^2$ for a Schwarzschild black hole, where the validity of the analysis requires that $t_{\text{coll}} \gg t_i$. The influence of the kink instability on the Poynting jet remains to be investigated.

We thank Alexander Koldoba and John Finn for valuable discussions and help with this work. Detailed comments by an anonymous referee were valuable for improving this Letter. This research was partially supported by NASA grants NAG5-6311 and NAG5-9047.

REFERENCES

- Aly, J. J. 1984, *ApJ*, 283, 349
 Begelman, M. C., Blandford, R. D., & Rees, M. J. 1984, *Rev. Mod. Phys.*, 56, 255
 Bell, A. R. 1994, *Phys. Plasmas*, 1, 1643
 Bisnovatyi-Kogan, G. S. 1993, in *Stellar Jets and Bipolar Outflows*, ed. L. Errico & A. A. Vittone (Dordrecht: Kluwer), 369
 Blandford, R. D. 1976, *MNRAS*, 176, 465
 ———. 1993, in *AIP Conf. Proc.* 280, *Compton Gamma-Ray Observatory*, ed. M. Friedlander, N. Gehrels, & D. J. Macomb (New York: AIP), 533
 Blandford, R. D., & Payne, D. G. 1982, *MNRAS*, 199, 883
 Bridle, A. H., & Eilek, J. A., eds. 1984, *Physics of Energy Transport in Extragalactic Radio Sources* (Greenbank: NRAO)
 Bührke, T., Mundt, R., & Ray, T. P. 1988, *A&A*, 200, 99
 Colgate, S. A., & Li, H. 2000, in *IAU Colloq. 195, Highly Energetic Physical Processes and Mechanisms for Emission from Astrophysical Plasmas*, ed. P. C. H. Martins, S. Tsuruta, & M. A. Weber (San Francisco: ASP), 255
 Eikenberry, S., Matthews, K., Morgan, E. H., Remillard, R. A., & Nelson, R. W. 1998, *ApJ*, 494, L61
 Gold, T., & Hoyle, F. 1960, *MNRAS*, 120, 7
 Koide, S., Meier, D. L., Shibata, K., & Kudo, T. 2000, *ApJ*, 536, 668
 Koldoba, A. V., Ustyugova, G. V., Romanova, M. M., Chechetkin, V. M., & Lovelace, R. V. E. 1995, *Ap&SS*, 232, 241
 Königl, A., & Ruden, S. P. 1993, in *Protostars and Planets III*, ed. E. H. Levy & J. Lunine (Tucson: Univ. Arizona Press), 641
 Krasnopolsky, R., Li, Z.-Y., & Blandford, R. D. 1999, *ApJ*, 526, 631
 Levinson, A. 1998, *ApJ*, 507, 145
 Lovelace, R. V. E. 1976, *Nature*, 262, 649
 Lovelace, R. V. E., Newman, W. I., & Romanova, M. M. 1997, *ApJ*, 484, 628
 Lovelace, R. V. E., Ustyugova, G. S., & Koldoba, A. V. 1999, in *IAU Symp. 194, Active Galactic Nuclei and Related Phenomena*, ed. Y. Terzian, D. W. Weedman, & E. E. Khachikian (San Francisco: ASP), 208
 Lovelace, R. V. E., Wang, J. C. L., & Sulkanen, M. E. 1987, *ApJ*, 315, 504
 Lynden-Bell, D. 1996, *MNRAS*, 279, 389
 Meier, D. L., Edgington, S., Godon, P., Payne, D. G., & Lind, K. R. 1997, *Nature*, 388, 350
 Mirabel, I. F., & Rodríguez, L. F. 1994, *Nature*, 371, 46
 Mundt, R. 1985, in *Protostars and Planets II*, ed. D. C. Black & M. S. Mathews (Tucson: Univ. Arizona Press), 414
 Newman, W. I., Newman, A. L., & Lovelace, R. V. E. 1992, *ApJ*, 392, 622
 Oyed, R., & Pudritz, R. E. 1997, *ApJ*, 482, 712
 Pudritz, R. E., & Norman, C. A. 1986, *ApJ*, 301, 571
 Romanova, M. M. 1999, in *IAU Symp. 194, Active Galactic Nuclei and Related Phenomena*, ed. Y. Terzian, D. W. Weedman, & E. E. Khachikian (San Francisco: ASP), 256
 Romanova, M. M., & Lovelace, R. V. E. 1997, *ApJ*, 475, 97
 Romanova, M. M., Ustyugova, G. V., Koldoba, A. V., Chechetkin, V. M., & Lovelace, R. V. E. 1997, *ApJ*, 482, 708
 ———. 1998, *ApJ*, 500, 703
 Sturrock, P. A. 1991, *ApJ*, 380, 655
 Ustyugova, G. V., Koldoba, A. V., Romanova, M. M., Chechetkin, V. M., & Lovelace, R. V. E. 1995, *ApJ*, 439, L39
 ———. 1999, *ApJ*, 516, 221

Note added in proof.—At the JENAM 2000 meeting in Moscow, 2000 June, Dr. J. Heyvaerts presented analytic results indicating the simultaneous formation of a collimated axial jet and an uncollimated outflow.